International Journal of Radiation Oncology biology • physics

www.redjournal.org

Biology Contribution

Improved Overall Survival of Mice by Reducing Lung Side Effects After High-Precision Heart Irradiation Using a Small Animal Radiation Research Platform

Wolfgang Sievert, PhD,* Stefan Stangl, PhD,* Katja Steiger, VMD,‡ and Gabriele Multhoff, PhD*,†

**Center of Translational Cancer Research, Technische Universität München (TranslaTUM), Campus Klinikum rechts der Isar, Department of Radiation Oncology, Klinikum rechts der Isar, Munich, Germany; †Institute of Pathology, Technische Universität München, Munich, Germany; ‡Institute of Innovative Radiotherapy, Helmholtz Zentrum München, Munich, Germany*

Received Sep 18, 2017, and in revised form Dec 14, 2017. Accepted for publication Feb 7, 2018.

Summary

The analysis of late radiation-induced heart disease is limited by a reduced overall survival of mice, induced by a co-irradiation of large portions of the lung. Therefore, an irradiation protocol was established that allows whole-heart irradiation with <10% co-irradiation of the lung (V16), which in turn enhances the survival of mice for at least 50 weeks after 16 Gy. The novel irradiation plan provides a

Purpose: The aim was to reduce radiation exposure of the lung in experimental models to increase overall survival of mice to study late radiation-induced heart disease.

Methods and Materials: A new irradiation plan was established on the Small Animal Radiation Research Platform machine for local heart irradiation of mice with single doses of 8 and 16 Gy. Lung damage was analyzed 20, 30, 40, and 50 weeks after irradiation by computed tomography scans and histology and compared with a sham-irradiated, age-matched, control group.

Results: The use of an 8 × 6-mm^2 collimator enabled local heart irradiation whereby only 18% of the lung received any irradiation. The V10 and V16 of the lung were 14% and 7%, respectively. After a mean heart dose of 8 and 16 Gy, mice survived for at least 50 weeks after irradiation. Computed tomography images demonstrated increased cell densities in the irradiated lung volume 50 weeks after irradiation. Concomitantly, histologic examination revealed fibrotic and inflammatory changes in the irradiated lung volume. In the heart, amyloid depositions and left ventricle hypertrophy were observed.

Conclusions: High-precision heart irradiation with 8 and 16 Gy using an 8 × 6-mm^2 beam induced cardiac amyloidosis and hypertrophy, which did not lead to myocardial dysfunction despite the presence of radiation pneumopathy in the small V16 of the exposed lung. By using the improved irradiation plan (V16: 7%), long-term survival of

Reprint requests to: Wolfgang Sievert, PhD, Center of Translational Cancer Research, Technische Universität München (TranslaTUM), Campus Klinikum rechts der Isar, Munich, Germany. Tel: (+49) 89-4140-6013; E-mail: wolfgang.sievert@tum.de

The work was supported by Bundesministerium für Bildung und Forschung Innovative therapies (01GU0823), Bundesministerium für Bildung und Forschung Kompetenzverbund Strahlenforschung (02NUK038A), and Bundesministerium für Wirtschaft und Energie (Arbeitsgemeinschaft industrieller Forschungsvereinigungen project GmbH, ZF4320102CS7), DFG SFB824/3, DFG STA1520/1-1.

Conflict of interest: none.

Int J Radiation Oncol Biol Phys, Vol. 101, No. 3, pp. 671–679, 2018

https://doi.org/10.1016/j.ijrobp.2018.02.017

promising tool for analyzing late radiation-induced heart diseases in mice.

the mice after heart irradiation can be achieved that allows clinically relevant experimental investigation of late radiation-induced heart disease effects.

Introduction

Radiation therapy of patients with thoracic tumors may induce delayed damage in healthy tissue, including the heart and lung. Although the volume exposure is kept as low as possible, parts of the heart and lung still may receive radiation doses above 20 Gy (1). Early pneumonitis is an inflammatory process that becomes clinically manifest after weeks. Late lung fibrosis follows months or years later in areas of the lung that were exposed to irradiation (2). In contrast, radiation-induced heart disease (RIHD) has a much longer latency. Myocardial fibrosis, cardiomyopathy, coronary artery disease, and valvular disease usually occur more than 10 to 15 years after radiation therapy (3). Depending on the irradiated subvolumes and dose distribution, subclinical radiation damage in the heart and lung may interact synergistically with respect to an increased morbidity. Experiments in rats showed that lung irradiation with 10 Gy reduced the tolerated dose to the heart and vice versa, contributing to cardiac or pulmonary dysfunction (4). The severity of signs and symptoms of pneumonitis is related to the irradiated volume and dose. The amount of lung volume that develops radiation-induced lung disease (RILD) is a critical parameter that defines the clinical tolerance of the lung. The percentage of lung volume that receives 20 Gy or more (V20) is a commonly used parameter to optimize the irradiation plan and to minimize the risk of RILD. In a non-small cell lung cancer (NSCLC) study no patient developed symptomatic grade 2 pneumonitis if the V20 was $<22\%$ (5). No radiation pneumonitis was observed in another study of NSCLC and SCLC patients with V20 of 20.1% (6).

As part of the EU-Cardiorisk project, RIHD was analyzed in preclinical studies after local heart irradiation with X ray. Collimation of the beams was usually performed using a lead plate, which covered the animal except for a window for heart irradiation. Often the whole thorax or large irradiation fields were used for whole-heart irradiation schemes (7). In mouse models, irradiation fields between 9×13 mm^2 and 10.6×15.0 mm^2 were used to ensure total heart irradiation. Because of the close neighborhood of heart and lung, up to 30% of the lung received 100% of the dose (8). Clinical signs of cardiac morbidity may be aggravated by functional interaction with RILD. The analysis of doses (<20 Gy) to the heart is limited by a reduced overall survival of mice at later time points: 38% of mice died spontaneously or had to be sacrificed between 30 and 40 weeks after 16 Gy local heart irradiation with a 30% lung co-irradiation (8). In a different study 40% of mice died 24 weeks and 90% of mice died 55 weeks after 16 Gy heart irradiation with a 20% lung co-irradiation (9). In other studies no survival data of mice were provided 60 weeks after heart irradiation with 16 Gy (10, 11). In contrast, no mouse died 39 weeks after a partial lung irradiation with 16 Gy when approximately 20% of the lung was irradiated (12).

The availability of an image guided Small Animal Radiation Research Platform (SARRP) allows high-precision irradiation on a millimeter scale (13). This device permits the exact targeting of the heart in a living mouse. Dose-volume histograms (DVHs) can be used to ensure whole-heart irradiation with minimal exposure of lung tissue. In this study a novel irradiation plan was established that allows total heart irradiation with 16 Gy with tolerated co-irradiation of the lung for at least 50 weeks.

Methods and Materials

Mice and irradiation procedure

Female C57Bl/6 mice (Charles River Laboratories, Sulzfeld, Germany) aged 10 to 14 weeks were randomly allocated to different treatment groups. Irradiation was performed using the high-precision image-guided SARRP (Xstrahl, Camberley, UK). Commissioning of the planning system was performed using a calibrated ionization chamber (International Atomic Energy Agency, Vienna, Austria; Technical Reports Series No. 398) and radiochromic films (Gafchromic EBT3, Ashland, Covington, KY), according to the manufacturer's recommendations. The output of the SARRP was regularly checked using a calibrated ionization chamber. Mice were anesthetized by isoflurane/oxygen inhalation for the duration of each treatment. Cone beam computed tomography (CBCT) using 60-kV and 0.8-mA photons filtered with aluminum (1 mm) was performed for each mouse to visualize the thorax. A total of 720 2-dimensional projections over 360° were used that provided 3 CT scans in transverse, sagittal, and frontal view. In each of the projections heart and lung were marked and fitted. The size of the beam was selected to cover the whole heart as marked before. A collimator in the exact size of the mouse heart was not present. Collimators were available with the following sizes: 1×1, 3×3, 5×5, 10×10, and 9×13 mm^2. The central axis of the beam was set in the isocenter of the heart, with a mean irradiation dose of 8 or 16 Gy. The heart was irradiated using 220-kV and 13-mA x-ray beams filtered with copper (0.15 mm). Control mice received sham irradiation (0 Gy). The software SARRP control and Muriplan were used to precisely target hearts and irradiation doses.

Separate groups of mice were irradiated for imaging and collecting hearts and lung at 20, 30, 40, and 50 weeks after irradiation. In total, 18, 20, and 26 mice received local heart irradiation with 0, 8, and 16 Gy, respectively. Animals were housed in single ventilated cages under pathogen-free conditions. Experiments were in agreement with national law on animal experiments and welfare and were performed in accordance with institutional guidelines.

In vivo imaging

Three mice of each irradiation group were imaged using the CT mode of the SARRP machine 20, 30, 40, and 50 weeks after irradiation. Mice were anesthetized by intraperitoneal injection of fentanyl (50 µg/kg body weight), medetomidine (500 µg/kg body weight), and midazolam (5 mg/kg body weight). The respiratory frequency and temperature were monitored during imaging. Cone beam CT was performed using 60-kV and 0.8-mA, and 720 2-dimensional projections were used to visualize the thorax in transverse, sagittal, and frontal view. The dose for CBCT was 2.4 cGy, and the field of view was 10×10 cm^2. Quantitative analysis of raw reconstructed images was performed by ImageJ (1.48v; National Institutes of Health, Bethesda, MD). Signal intensities (mean pixel value) of the CTs in transverse view were quantified using regions of interest (ROIs), which were placed manually into the pictures according to the isodoses of irradiated lung volume.

Histology and immunohistochemistry

The exact delivery of the irradiation beam was confirmed using the DNA damage repair marker γH2AX (Cell Signaling Technology, Danvers, MA) on a Bond Rx staining machine (Leica Biosystems, Nussloch, Germany) using a Polymer Refine detection system without postprimary reagent. Heart and lung of 3 animals were removed 1 hour after irradiation with 16 Gy. For each dose and time point hearts and lungs (n = 3 per group) were removed to investigate long-term radiation effects and anatomic changes. Tissue was fixed in formalin overnight and embedded in paraffin. Blocks were sectioned in 2-µm slices and stained with eosin (eosin y-solution 0.5% aqueous) and hematoxylin (Mayer's hematoxylin) to visualize tissue structure according to standard protocols. Elastica van Gieson staining was performed with Resorcin (Waldeck, Muenster, Germany) fuchsin solution (20 minutes), differentiation in 96% alcohol, Weigerts iron hematoxylin staining solution (8 minutes), and Picrofuchsin (Sigma, Darmstadt, Germany) solution (2 minutes) to determine the extent of collagen, indicative for fibrosis. To differentiate hyaline depositions observed within the myocardium, a Congo red staining was performed with Congo red solution (30 minutes) counterstained with Mayer's hematoxylin. All slices were scanned with a digital slide scanner (Leica AT2) to create digital images. Quantitative analysis of cell density was performed by ImageJ (1.48v) using hematoxylin and eosin staining. Pictures were converted to gray-scale and set to the binary system. Lung subvolumes were quantified using ROIs, which were placed manually into the pictures in the cranial portions of the lung lobes. Pulmonary alterations were scored semi-quantitatively with a histopathologic scoring system modified according to Jackson et al (14). The following parameters were evaluated for the irradiated as well as the unirradiated lung area by an experienced pathologist (KS): activation of bronchus-associated lymphoid tissue, intra-alveolar infiltration, interstitial fibrosis, perivascular infiltration, hyperemia/bleeding, and the occurrence of an acidophilic macrophage pneumonia. All parameters were scored with a 4-tier scoring system (0-3).

Myocardial lesions were determined on the basis of a pathologic scoring system for chronic cardiotoxicity (15). An experienced pathologist (KS) evaluated hematoxylin and eosin−stained sections of the heart using ImageScope (Leica Biosystems, Nussloch, Germany) software on electronic slides. Left ventricular hypertrophy was measured on central longitudinal heart slices.

Statistical analysis

Comparative analysis of the data was carried out using a nonparametric test (Mann-Whitney). The significance levels were $P < .05$ (5%) and $P < .01$ (1%). Data were presented as means of the number of mice in the respective result.

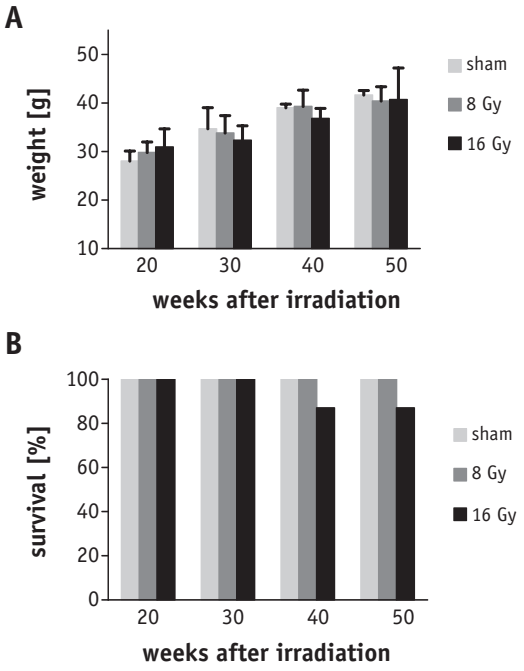

Fig. 1. Weights and survival of mice. (A) The weights of mice showed no significant changes up to 50 weeks after 8 and 16 Gy irradiation compared with sham mice. (B) All mice (except 2 mice between 35 and 37 weeks) appeared healthy up to 50 weeks after irradiation.

Results

Mouse survival

Up to 50 weeks after irradiation with 8 and 16 Gy, no significant differences in weight were observed compared with sham-irradiated mice (Fig. 1A). Up to 20 and 30 weeks after irradiation, all mice appeared healthy (Fig. 1B). Two mice had to be killed between week 35 and 37 owing to poor health condition after 16 Gy heart irradiation. Both lungs showed pathologic changes in the irradiated and unirradiated volume (data not shown). Both mice were pathologically diagnosed with lymphoblastic lymphoma with generalized lymphadenopathy and splenomegaly due to infiltration of lymph nodes, spleen, and lung (in 1 animal) with CD45R (B220)-positive lymphoblasts (data not shown). The findings in both cases were consistent with a Burkitt-like lymphoma (mature B-cell lymphoma with lymphoblastic morphology [16]), which is a systemic disease. On the one hand it is known that irradiation can cause or accelerate the development of lymphoma; on the other hand aged C57Bl/6 mice often develop lymphoma (17, 18). Therefore, an indirect effect of irradiation cannot be completely excluded, but a direct effect of lung irradiation as the primary cause of disease is very unlikely. The remaining mice (n = 9, sham; n = 11, 8 Gy; n = 12, 16 Gy) appeared healthy for the duration of the study up to 50 weeks (Fig. 1B).

Precision heart irradiation

Several beam directions and field sizes were tested, and DVHs were calculated for heart and lung. In each irradiation protocol the heart should be irradiated with a

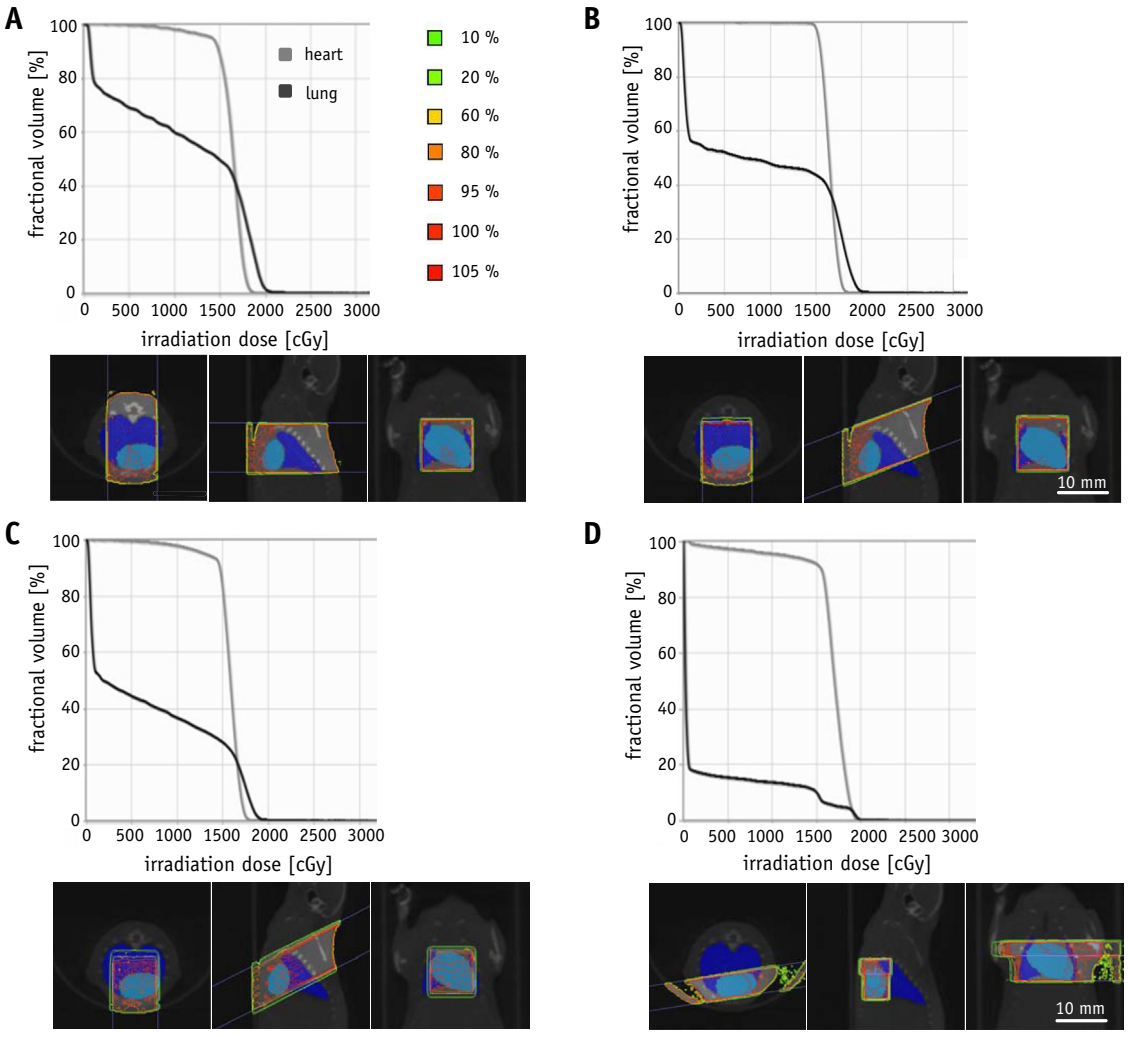

Fig. 2. Dose-volume histograms of 4 different dose plans for whole-heart irradiation with 16 Gy. Dose-volume histograms of 4 different beams and the computed tomography pictures in transverse, sagittal, and frontal view are shown. (A) A single posterior–anterior beam (13 × 9 mm^2) results in whole-heart irradiation. The V10 and V16 of the lung were 60% and 45%. (B) The same beam (13 × 9 mm^2) using an angle of 20° shows also whole-heart irradiation. The V10 and V16 were 48% and 42%. (C) Using a posterior–anterior beam (9 × 8 mm^2) the whole heart receives irradiation. The V10 and V16 were 37% and 28%. (D) A lateral beam (8 × 6 mm^2) results in 95% heart irradiation. The V10 and V16 were 14% and 7%.

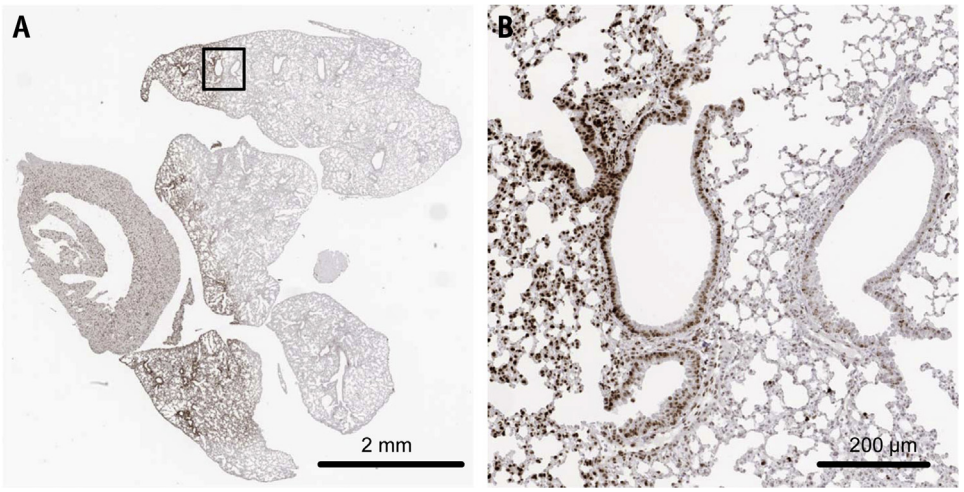

Fig. 3. Immunohistochemical γH2AX staining of heart and lung. (A) The use of the 8 × 6-mm^2 beam shows positive staining in the whole heart and in cranial parts of the lung lobes close to the heart. (B) The beam edge is very sharp and can be visualized by γH2AX immunohistochemistry.

mean target dose of 16 Gy, with minimal exposure of lung tissue. First a posterior–anterior beam was tested between the regular sizes of 9 × 13 mm^2 and 10.6 × 15.0 mm^2. Using the 9 × 13-mm^2 beam (couch angle: 0°; gantry angle: 0°) the percentage of lung volume that received 10 Gy or more (V10) was approximately 60%, and the volume that received 16 Gy or more (V16) was 45% (Fig. 2A). For a better lung protection, the 9 × 13-mm^2 beam was tested in a different angle (couch angle: 90°; gantry angle: 25°). In this case V10 and V16 were still 48% and 42%, respectively (Fig. 2B). Using the smallest posterior–anterior beam of 8 × 9 mm^2 (couch angle: 90°; gantry angle: 25°) that covered the whole heart, V10 and V16 decreased to 37% and 28%, respectively (Fig. 2C). However, using a lateral 6 × 8-mm^2 beam (couch angle: 0°; gantry angle: 100°), V10 and V16 dropped to 14% and 7%, respectively (Fig. 2D). Only 18% of the total lung volume was exposed to irradiation. For the irradiation this beam was composed of 3 single beams (5 × 5, 3 × 3, and 3 × 3 mm^2), which were put together without any overlap. For simplicity the beam size was referred to as 6 × 8 mm^2, although one length consists partly of 5-mm and 6-mm (3 + 3 mm) breadth instead of continuously 6 mm (Fig. 2D). This irradiation plan with 3 lateral beams was used for all mice in the present study. For simplicity the irradiation doses were referred to as 8 and 16 Gy instead of the measured doses of 8.1 ± 0.1 and 16.2 ± 0.3.

To validate the precision of heart irradiation by the 8 × 6-mm^2 beam, sections of heart and lung were analyzed by γH2AX staining. The whole heart showed positive foci, whereas small parts of lung close to the heart also received irradiation (Fig. 3A). Despite the breathing motion the beam edge was very sharp (Fig. 3B).

Noninvasive heart and lung imaging

Micro-CT imaging was used to examine evidence for fibrotic changes. For the quantitative analysis the ROI was manually inserted into the CT images taken from 3 mice at 20, 30, 40, and 50 weeks. The ROI included the lung tissue exposed to the prescribed doses but excluded the heart (Fig. 4A). Visible signal analysis of CT pictures showed a faint increase of lung density after 8 Gy and a distinct increase after 16 Gy at 50 weeks (Fig. 4A). Quantitative analysis of the CT images indicated a significant increase of the mean pixel value of ROI 40 and 50 weeks after 8 Gy (50,000 and 50,210; $P < .029$ and $P < .029$) and a significant increase of mean pixel value of ROI 40 and 50 weeks after 16 Gy (50,190 and 50,290; $P < .029$ and $P < .029$) compared with control mice (49,730 and 49,740) (Fig. 4B).

Histopathology of irradiated hearts and lungs

Hearts and lungs of irradiated and control mice were examined for evidence of pathologic alterations. Hematoxylin and eosin staining showed clear differences in irradiated and sham-irradiated control mice after 50 weeks. The control lung showed a healthy dense network of alveolae (Fig. 5A). In contrast, the lungs of the mice irradiated with 8 and 16 Gy displayed intra-alveolar accumulation of macrophages (foam cells) and intra-alveolar edema in the cranial (pericardially located) portions of the lung lobes. One animal showed an acidophilic macrophage pneumonia. Quantitative analysis of the pictures indicated a significant increase of cell density 50 weeks after 8 Gy (62%; $P = .002$) and 16 Gy (69%, $P = .002$) compared with control mice (28%) (Fig. 5B).

Elastica van Gieson staining and morphologic quantification showed slight interstitial fibrosis in the irradiated

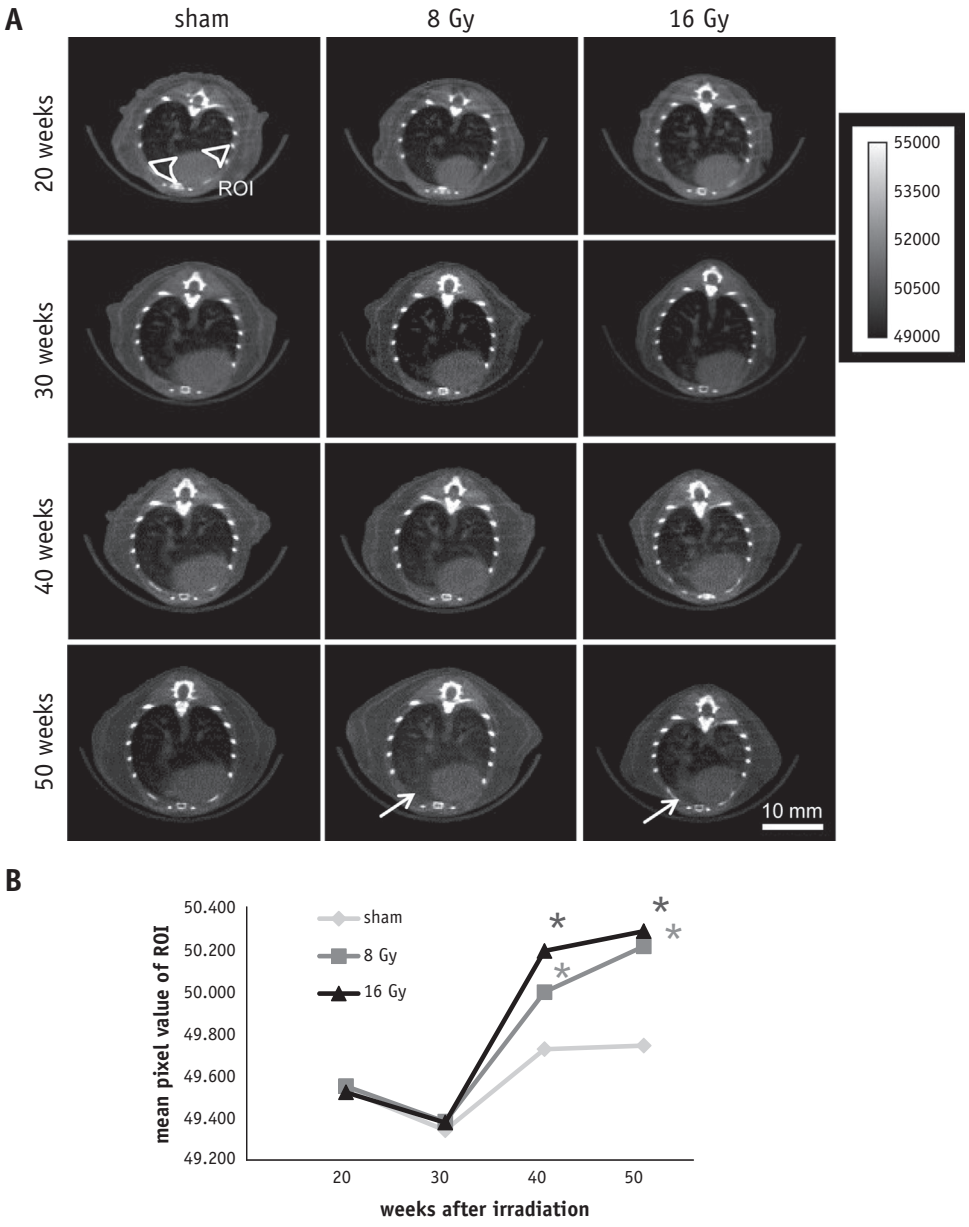

Fig. 4. Cone beam computed tomography (CT) of mouse thorax 20, 30, 40, and 50 weeks after sham, 8 Gy, and 16 Gy heart irradiation. (A) The CT pictures show a faint increase of lung density after 8 Gy and a distinct increase after 16 Gy at 50 weeks (arrows). (B) Quantitative analysis of the CT images indicates a significant increase of the mean pixel value of the region of interest (ROI) 40 and 50 weeks after 8 Gy and 16 Gy compared with control mice. *Significantly different values ($P < .05$).

lung volume 50 weeks after 8 and 16 Gy (Fig. 6A, Table 1). Moreover, a slight to moderate mixed perivascular infiltration was observed for both doses after 50 weeks (Fig. 6B, Table 1).

In the heart, doses of 8 and 16 Gy resulted in multifocal amyloidosis in the myocardium as well as a left ventricular hypertrophy (Fig. 6C, Table 1). Apart from multifocal amyloidosis no further lesions according to the scoring system of Rahman et al (15) were determined as a long-term effect. Left ventricular hypertrophy was detected on central longitudinal heart slices. An increase in left ventricular lumen and ventricular wall thickness was observed.

Discussion

High-precision heart irradiation with minimal exposure of the surrounding lung tissue is important to increase overall survival of mice to be able to study late RIHD effects. Survival of the mice is limited by RILD (pneumonitis and late fibrosis) if the irradiated lung volume exceeds a critical value. In many preclinical studies, the DVH of heart and lung has not been reported. Proton irradiation of 25% of the lung with 20 Gy had no effect on breathing rate, whereas 50% lung irradiation induced not only a significant increase

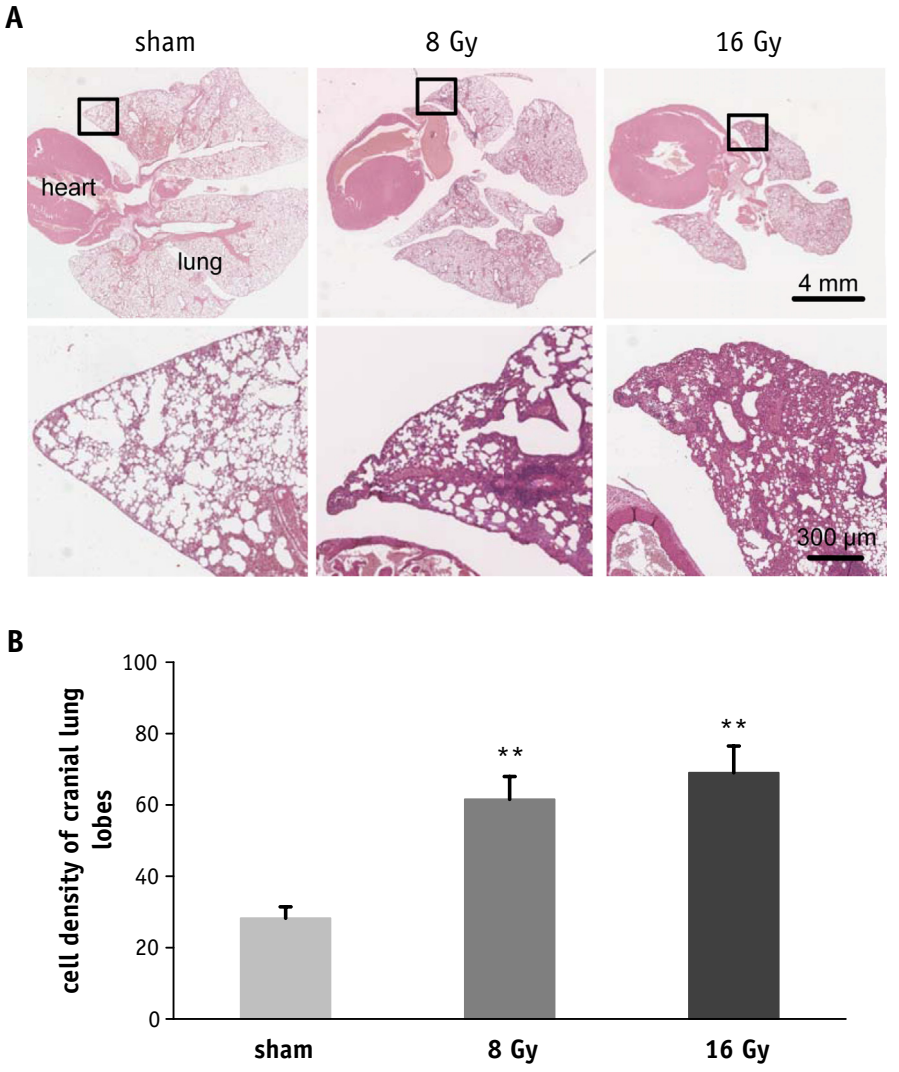

Fig. 5. Hematoxylin and eosin staining of heart and lung 50 weeks after sham, 8 Gy, and 16 Gy heart irradiation. (A) The upper row shows a section of heart and lung at low magnification 50 weeks after sham, 8 Gy, and 16 Gy. The lower row shows the subvolumes at higher magnification marked by a square in the upper pictures, which was in the radiation beam. The sham-irradiated animal shows a normal histology of lung and heart. Irradiation with 8 Gy leads to slight to moderate perivascular infiltration. After 16 Gy, intra-alveolar edema and accumulation of macrophages in the alveolar lumina are observed. (B) The quantified tissue percentage of irradiated lung indicated a significant increase 50 weeks after 8 and 16 Gy compared with control mice. **Significantly different values ($P < .01$).

in breathing rate but also pulmonary hypertension, leading to right ventricle systolic pressure overload and right ventricle hypertrophy 8 weeks after irradiation (4). With decreasing irradiated lung subvolume, the tolerance dose for RILD increased 8 weeks after irradiation, whereas inflammation and fibrosis increased 26 weeks later (19). Mouse studies using X rays on different lung subvolumes after 16 Gy at different time points are rare. Local heart irradiation with 30% lung co-irradiation showed a symptom-free survival up to 16 weeks after 16 Gy but a reduced survival (62% survivors) after 40 weeks (8, 20). Heart irradiation with 20% lung co-irradiation resulted in 10% survivors after 55 weeks (9). The present study demonstrates that if only <10% of the lung volume is exposed to 16 Gy, the survival of mice was increased to at least 50 weeks after 16 Gy heart irradiation, although increased cell density in the irradiated lung subvolume showed clear signs of radiation pneumopathy. This indicates that lung alteration in approximately 10% of the lung volume can be compensated and functional damage can be avoided for at least 50 weeks after irradiation. The compensation of this subvolume for earlier periods is also shown in a study that analyzed dose-volume effects in mouse lung (21). No increase in breathing rate was observed 22 weeks after 19% lung irradiation, even after a dose of 22 Gy. Further, it was shown that a subvolume in the apex of lung is less radiosensitive than the same subvolume in the base. Irradiation of 84% of the lung in the

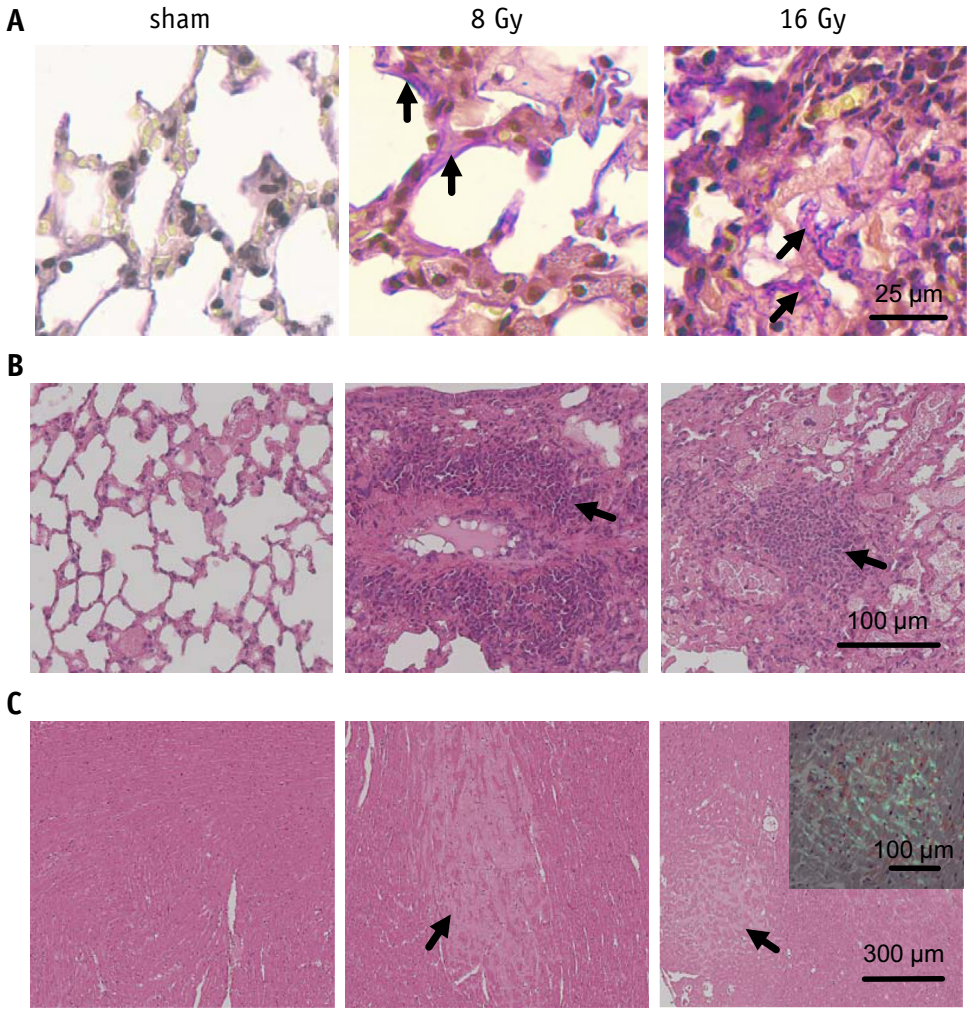

Fig. 6. Elastica van Gieson and hematoxylin and eosin staining of heart and lung 50 weeks after sham, 8 Gy, and 16 Gy heart irradiation. (A) Elastica van Gieson staining shows slight interstitial fibrosis in irradiated lung subvolume 50 weeks after 8 Gy and 16 Gy (arrows). (B) Hematoxylin and eosin staining illustrate a mixed perivascular infiltration in irradiated lung subvolume 50 weeks after 8 Gy and intra-aveolar edema and macrophages (foam cells) after 16 Gy (arrows). (C) Hematoxylin and eosin staining indicates amyloid deposition in the heart verified by Congo red staining (inset) 50 weeks after 8 Gy and 16 Gy (arrows).

apex or in the base with 16 Gy resulted in 17% lethality in those mice irradiated to the apex and in 73% lethality in mice irradiated to the base after 32 weeks. The authors suggested that the different radiation sensitivity of the lung is based on heterogeneous distribution of alveoli (21). Large volumes of the apex are occupied by major airways and less sensitive gas exchange units, whereas the base shows the opposite. The different sensibility of the lung might also play a role in this study to enhance the symptom-free survival of mice up to 50 weeks after irradiation.

Table 1 Incidence of interstitial fibrosis, perivascular infiltration of macrophages, and heart hyaline depositions 50 weeks after irradiation

Variable	Sham	8 Gy	16 Gy
Intra-alveolar foam cells	0-1	1	1-2
Lung interstitial fibrosis	0	0-1	1
Lung perivascular infiltration of macrophages	0	1-2	1-2
Heart hyaline depositions (%)	0	5	15-25

Pulmonary alterations (n = 3) were scored semi-quantitatively with a histopathologic scoring system. All parameters were scored with a 4-tier scoring system (0-3). Myocardial lesions (n = 3) were evaluated on hematoxylin and eosin–stained sections and quantified semi-quantitatively.

Cardiac amyloidosis and hypertrophy were shown 40 weeks after heart irradiation with 16 Gy. In this study the survival of mice was approximately 60% (9). With the new irradiation protocol nearly 100% of the mice survived for at least 50 weeks after irradiation, with minor symptoms such as cardiac amyloidosis and a weak hypertrophy.

The damage of heart and lung endothelial cells was investigated between 5 and 20 weeks after thorax irradiation with 8 Gy (7, 22). The study showed that the cell surface marker intercellular adhesion molecule-1 and

vascular cell adhesion molecule-1 were persistently increased starting from 10 up to 20 weeks after 8 Gy. The new irradiation plan allows the analysis of late RIHD with a minimum contribution of RILD. In particular, the influence of intercellular adhesion molecule-1 and vascular cell adhesion molecule-1 to endothelial cell damage after heart irradiation can be analyzed for higher irradiation doses and later time points.

Conclusions

A novel irradiation plan was established using an image guided small animal radiation platform for whole-heart irradiation with <10% co-irradiation of the lung. Despite the presence of pulmonary fibrosis and inflammation in this small lung subvolume, irradiated mice survived symptom-free for at least 50 weeks. This indicates that the development of inflammatory (pneumonitis) and fibrotic changes in such small lung volumes can be compensated, and therefore functional interaction between subclinical radiation damage in lung and heart can be avoided. The new irradiation plan provides a promising tool for further preclinical studies analyzing RIHD in mice.

References

1. Andratschke N, Maurer J, Molls M, et al. Late radiation-induced heart disease after radiotherapy. Clinical importance, radiobiological mechanisms and strategies of prevention. *Radiother Oncol* 2011;100:160-166.
2. McDonald S, Rubin P, Phillips TL, et al. Injury to the lung from cancer therapy: Clinical syndromes, measurable endpoints, and potential scoring systems. *Int J Radiat Oncol Biol Phys* 1995;31:1187-1203.
3. Darby SC, Cutter DJ, Boerma M, et al. Radiation-related heart disease: Current knowledge and future prospects. *Int J Radiat Oncol Biol Phys* 2010;76:656-665.
4. Ghobadi G, van der Veen S, Bartelds B, et al. Physiological interaction of heart and lung in thoracic irradiation. *Int J Radiat Oncol Biol Phys* 2012;84:e639-e646.
5. Graham MV, Purdy JA, Emami B, et al. Clinical dose-volume histogram analysis for pneumonitis after 3D treatment for non-small cell lung cancer (NSCLC). *Int J Radiat Oncol Biol Phys* 1999;45:323-329.
6. Tsujino K, Hirota S, Endo M, et al. Predictive value of dose-volume histogram parameters for predicting radiation pneumonitis after concurrent chemoradiation for lung cancer. *Int J Radiat Oncol Biol Phys* 2003;55:110-115.
7. Sievert W, Trott KR, Azimzadeh O, et al. Late proliferating and inflammatory effects on murine microvascular heart and lung endothelial cells after irradiation. *Radiother Oncol* 2015;117:376-381.
8. Seemann I, Gabriels K, Visser NL, et al. Irradiation induced modest changes in murine cardiac function despite progressive structural damage to the myocardium and microvasculature. *Radiother Oncol* 2012;103:143-150.
9. Monceau V, Llach A, Azria D, et al. Epac contributes to cardiac hypertrophy and amyloidosis induced by radiotherapy but not fibrosis. *Radiother Oncol* 2014;111:63-71.
10. Walaszczyk A, Szoltysek K, Jelonek K, et al. Heart irradiation reduces microvascular density and accumulation of HSPA1 in mice. *Strahlenther Onkol* 2018;194:235-242.
11. Patties I, Haagen J, Dorr W, et al. Late inflammatory and thrombotic changes in irradiated hearts of C57BL/6 wild-type and atherosclerosis-prone ApoE-deficient mice. *Strahlenther Onkol* 2015;191:172-179.
12. Granton PV, Dubois L, van Elmpt W, et al. A longitudinal evaluation of partial lung irradiation in mice by using a dedicated image-guided small animal irradiator. *Int J Radiat Oncol Biol Phys* 2014;90:696-704.
13. Verhaegen F, Granton P, Tryggestad E. Small animal radiotherapy research platforms. *Phys Med Biol* 2011;56:R55-R83.
14. Jackson IL, Xu P, Hadley C, et al. A preclinical rodent model of radiation-induced lung injury for medical countermeasure screening in accordance with the FDA animal rule. *Health Phys* 2012;103:463-473.
15. Rahman A, More N, Schein PS. Doxorubicin-induced chronic cardiotoxicity and its protection by liposomal administration. *Cancer Res* 1982;42:1817-1825.
16. Morse HC 3rd, Anver MR, Fredrickson TN, et al. Bethesda proposals for classification of lymphoid neoplasms in mice. *Blood* 2002;100:246-258.
17. Kominami R, Niwa O. Radiation carcinogenesis in mouse thymic lymphomas. *Cancer Sci* 2006;97:575-581.
18. Ward JM. Lymphomas and leukemias in mice. *Exp Toxicol Pathol* 2006;57:377-381.
19. van der Veen SJ, Faber H, Ghobadi G, et al. Decreasing irradiated rat lung volume changes dose-limiting toxicity from early to late effects. *Int J Radiat Oncol Biol Phys* 2016;94:163-171.
20. Azimzadeh O, Sievert W, Sarioglu H, et al. PPAR alpha: a novel radiation target in locally exposed Mus musculus heart revealed by quantitative proteomics. *J Proteome Res* 2013;12:2700-2714.
21. Travis EL, Liao ZX, Tucker SL. Spatial heterogeneity of the volume effect for radiation pneumonitis in mouse lung. *Int J Radiat Oncol Biol Phys* 1997;38:1045-1054.
22. Sievert W, Tapio S, Breuninger S, et al. Adhesion molecule expression and function of primary endothelial cells in benign and malignant tissues correlates with proliferation. *PLoS One* 2014;9:e91808.